BIOCHEMISTRY
including biophysical chemistry & molecular biology

Article

pubs.acs.org/biochemistry

Biochemical and Structural Analysis of RraA Proteins To Decipher Their Relationships with 4-Hydroxy-4-methyl-2-oxoglutarate/4-Carboxy-4-hydroxy-2-oxoadipate Aldolases

Scott Mazurkewich, Weijun Wang, and Stephen Y. K. Seah*

Department of Molecular and Cellular Biology, University of Guelph, Guelph, Ontario, Canada N1G 5E9

Supporting Information

ABSTRACT: 4-Hydroxy-4-methyl-2-oxoglutarate (HMG)/4-carboxy-4-hydroxy-2-oxoadipate (CHA) aldolases are class II (divalent metal ion dependent) pyruvate aldolases from the *meta* cleavage pathways of protocatechuate and gallate. The enzyme from *Pseudomonas putida* F1 is structurally similar to a group of proteins termed regulators of RNase E activity A (RraA) that bind to the regulatory domain of RNase E and inhibit the ribonuclease activity in certain bacteria. Analysis of homologous RraA-like proteins from varying species revealed that they share sequence conservation within the active site of HMG/CHA aldolase. In particular, the *P. putida* F1 HMG/CHA aldolase has a D-X_{20}-R-D motif, whereas a G-X_{20}-R-D-X_2-E/D motif is observed in the structures of the RraA-like proteins from *Thermus thermophilus* HB8 (*Tt*RraA) and *Saccharomyces cerevisiae* S288C (Yer010Cp) that may support metal binding. *Tt*RraA and Yer010Cp were found to contain HMG aldolase and oxaloacetate decarboxylase activities. Similar to the *P. putida* F1 HMG/CHA aldolase, both *Tt*RraA and Yer010Cp enzymes required divalent metal ions for activity and were competitively inhibited by oxalate, a pyruvate enolate analogue, suggesting a common mechanism among the enzymes. The RraA from *Escherichia coli* (*Ec*RraA) lacked detectable C−C lyase activity. Upon restoration of the G-X_{20}-R-D-X_2-E/D motif, by site-specific mutagenesis, the *Ec*RraA variant was able to catalyze oxaloacetate decarboxylation. Sequence analysis of RraA-like gene products found across all the domains of life revealed conservation of the metal binding motifs that can likely support a divalent metal ion-dependent enzyme reaction either in addition to or in place of the putative RraA function.

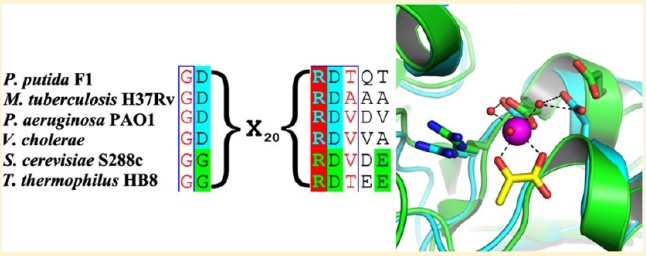

The 4-hydroxy-4-methyl-2-oxoglutarate (HMG)/4-carboxy-4-hydroxy-2-oxoadipate (CHA) aldolase is the final enzyme found in both the protocatechuate and gallate *meta* cleavage pathways of aromatic degrading bacteria such as *Pseudomonas putida* and *Sphingomonas paucimobilis*.[1−3] The enzyme is a class II, divalent metal ion-dependent, pyruvate aldolase that catalyzes the aldol cleavage of HMG and CHA into two molecules of pyruvate in the former and a molecule of each pyruvate and oxaloacetate (OAA) in the latter (Scheme 1).[4] The enzyme also contains a secondary OAA decarboxylase activity due to the common pyruvate enolate transition state formed following carbon−carbon (C−C) bond cleavage in the retro-aldol and decarboxylase reactions.[5] The first structure of an HMG/CHA aldolase (from *P. putida* F1) was recently determined by X-ray crystallography and was found to contain an $\alpha\beta\beta\alpha$ sandwich fold that is structurally distinct from previously identified class II pyruvate aldolases such as DmpG, HsaF, and HpaI.[5−8] Instead, the HMG/CHA aldolase is structurally similar to a group of proteins named regulators of RNase E activity A (RraA).

First characterized in *Escherichia coli*, RraA binds to RNase E and inhibits its ribonuclease activity.[9] RNase E is the principal component of the multiprotein complex called the RNA degradosome and is the major endoribonuclease controlling mRNA stability in *E. coli*.[10] RNase E contains an N-terminal catalytic domain and a C-terminal regulatory domain that acts as a binding scaffold for several proteins, including ATP-dependent DEAD-box RNA helicase (RhlB), enolase, and polynucleotide phosphorylase. *E. coli* RraA (*Ec*RraA) binds in two locations on the RNase E regulatory scaffold, the RNA binding domain (RBD) and arginine-rich domain 2 (AR2), preventing RNA transcripts from interacting with the scaffold.[11] *Ec*RraA can also interact directly with DEAD-box RNA helicases such as RhlB, RhlE, and SrmB, resulting in inhibition of ATP turnover in the helicases.[11,12] RhlB is required for processing of RNA containing secondary structural elements to allow for complete degradation of transcripts by the degradosome.[13] Thus, *Ec*RraA affects RNA metabolism by modulation of not only RNase E but also the RNA helicases.

*Ec*RraA [Protein Data Bank (PDB) entry 1Q5X], although similar in structure to HMG/CHA aldolase, is shorter at both the N-terminus and the C-terminus by approximately 30 residues.[14] The protein is therefore missing one of the key ligands for metal cofactor binding found in the HMG/CHA aldolase.[5,14]

Received: November 1, 2013
Revised: December 18, 2013
Published: December 20, 2013

dx.doi.org/10.1021/bi401486g | *Biochemistry* 2014, 53, 542−553

Scheme 1. Aldol Cleavage Catalyzed by the HMG/CHA Aldolase[a]

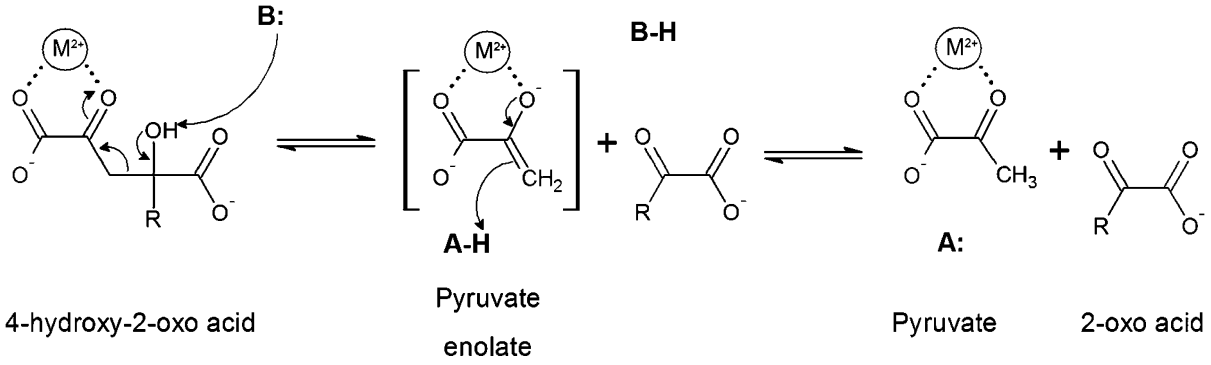

[a]For HMG, the R group is -CH_3, which yields 2 mol of pyruvate, and for CHA, the R group is -CH_2COO^-, which yields 1 mol each of pyruvate and oxaloacetate.

Structures of homologous RraA-like proteins from *Geobacillus kaustophilus* HTA426 (PDB entry 2PCN), *Mycobacterium tuberculosis* H37Rv (PDB entry 1NXJ), *Pseudomonas aeruginosa* PA01 (PDB entry 3C8O), *Pseudomonas syringae* pv. *tomato* str. DC3000 (PDB entry 3K4I), *Vibrio cholerae* (PDB entry 1VI4), *Saccharomyces cerevisiae* S288C (PDB entry 2C5Q), and *Thermus thermophilus* HB8 (PDB entry 1J3L) have all been deposited in the PDB.[15−18] To date, only *Ec*RraA and a RraA protein from *Vibrio vulnificus* have been determined to have RNase E binding and inhibitory function, although several gene records that are minimally identical in sequence to *Ec*RraA are annotated as being an RraA.[11,19] The lack of a defined RNase E or degradosome in some of these species, such as in *T. thermophilus* HB8 and *S. cerevisiae* S288C, raises questions regarding the functions of these proteins. It has also not been determined if any of the RraA-like proteins possess enzymatic activities similar to that of the HMG/CHA aldolase.

Herein we report the characterization of aldolase activity in *Ec*RraA, the putative RraA from *T. thermophilus* HB8 (*Tt*RraA), and the homologue from *S. cerevisiae* S288C (Yer010Cp). We have shown that both *Tt*RraA and Yer010Cp contain HMG aldolase and OAA decarboxylase activities while *Ec*RraA is enzymatically inactive. Structural analyses have revealed minimal motifs required for divalent metal ion binding necessary to support enzymatic activity. Substitution of key residues to restore one of these motifs was sufficient to rescue *Ec*RraA C−C lyase activity. Homologous gene products of the RraA-like proteins were identified in all domains of life, with many containing the conserved minimal motif identified here as a prerequisite for enzymatic activity. The results provide a framework for the correct functional annotation of this widely distributed family of proteins.

EXPERIMENTAL PROCEDURES

Chemicals. Sodium pyruvate, sodium oxalate, oxaloacetic acid, L-lactate dehydrogenase (LDH, rabbit muscle), and Dowex 1X8-200 ion exchange resin were from Sigma-Aldrich (Oakville, ON). Restriction enzymes and Pfu polymerase were from Invitrogen (Burlington, ON) or New England Biolabs (Pickering, ON). All other chemicals were analytical grade and were obtained from either Sigma-Aldrich or Fisher Scientific (Nepean, ON).

DNA Manipulations. Plasmid pET-11a harboring the TTHA1322 gene from *T. thermophilus* HB8 was obtained from the RIKEN Bioresource Centre.[20] Plasmid pET-9a harboring the Yer010c gene from *S. cerevisiae* S288C was obtained from N. Leulliot (Université Paris-Sud, Orasay, France).[16] This pET-9a-Yer010c construct was modified by the introduction of a stop codon before the plasmid-encoded C-terminal histidine tag by site-specific mutagenesis to allow for expression of the untagged gene. *Ec*RraA was amplified from genomic DNA and inserted into plasmid pT7-7[21] using primers containing NdeI and HindIII restriction sites at the 5′ and 3′ ends, respectively.

Gene mutations to create the D75G/A76G/E77N/Q98D *Ec*RraA variant and the HMG/CHA aldolase E199A variant were introduced by site-specific mutagenesis using the modified Quikchange method.[22] Primers utilized are listed in Table 1 of the Supporting Information. All modified plasmids were transformed into *E. coli* DH5α for propagation, and the gene mutations were confirmed by DNA sequencing at the Guelph Molecular Supercenter (University of Guelph).

Expression and Purification of the HMG/CHA Aldolase, Yer010Cp, *Tt*RraA, and *Ec*RraA. The expression and purification of the wild type (WT) and E199A variant of the HMG/CHA aldolase were as previously described.[5] Recombinant *E. coli* BL21(λDE3) harboring a plasmid encoding either TTHA1322 (*Tt*RraA) from *T. thermophilus* HB8, ECU56082 (*Ec*RraA) from *E. coli*, or Yer010Cp from *S. cerevisiae* S288C was propagated in 1 L of Luria-Bertani medium containing either 100 μg/mL ampicillin for *Ec*RraA and *Tt*RraA or 34 μg/mL kanamycin for Yer010Cp at 37 °C until a density of 0.6 at 600 nm wavelength was reached. In each case, protein expression was induced by the addition of 0.5 mM IPTG and the cultures were incubated at 15 °C overnight before being harvested by centrifugation at 5000*g* for 10 min.

Chromatography was performed on an ÄKTA Explorer 100 instrument (Amersham Pharmacia Biotech, Baie d'Urfé, QC). Buffers containing 20 mM sodium HEPES (pH 7.5) were used throughout each purification procedure unless indicated otherwise. Each cell pellet was resuspended in buffer and disrupted with a French press. The cell debris was removed by centrifugation (17500*g* for 15 min), and the supernatants were filtered through a 0.45 μm filter.

For the purification of *Ec*RraA, the supernatant was loaded onto a Source 15Q (Amersham Pharmacia Biotech) anion exchange column (2 cm × 13 cm). The column was washed with 2 column volumes of the buffer containing 0.4 M NaCl followed by a linear gradient of NaCl from 0.4 to 0.6 M over 12 column volumes. The *Ec*RraA protein eluted with approximately 0.5 M NaCl. Fractions containing *Ec*RraA were concentrated to ∼2 mL by ultrafiltration with a YM10 filter (Millipore, Nepean, ON).

dx.doi.org/10.1021/bi401486g | *Biochemistry* 2014, 53, 542−553

The concentrated protein was then loaded on a HiLoad 26/60 Superdex 200 prep gel filtration column (Amersham Pharmacia Biotech) and eluted with buffer containing 0.15 M NaCl. The purified protein was concentrated to 10 mg of protein/mL as before, aliquoted, and stored at −80 °C in 20 mM sodium HEPES buffer (pH 7.5).

For the purification of *Tt*RraA, the crude extract was separated by an anion exchange column as described for *Ec*RraA, except a linear gradient of 0.10 to 0.30 M over 12 column volumes was used. *Tt*RraA eluted with approximately 0.20 M NaCl. Active fractions were pooled and concentrated to approximately 40 mL by ultrafiltration, and the clear supernatant was heat treated at 75 °C for 10 min and the denatured protein was removed by centrifugation (17500*g* for 10 min). The extract was concentrated to ∼2 mL by ultrafiltration and purified by gel filtration as described for *Ec*RraA. The purified enzyme was concentrated to 10 mg of protein/mL via ultrafiltration, aliquoted, and stored at −80 °C in 20 mM sodium HEPES buffer (pH 7.5).

For the purification of Yer010Cp, the crude extract was separated by an anion exchange column as described for *Ec*RraA, except a linear gradient of 0.0 to 0.25 M over 12 column volumes was used. The Yer010Cp protein eluted with approximately 0.15 M NaCl. Active fractions were pooled and concentrated to approximately 5 mL by ultrafiltration, and the clear supernatant was loaded onto a Phenyl Sepharose hydrophobic interaction chromatography column (1 cm × 18.5 cm) and purified with a 6 column volume linear gradient of ammonium sulfate from 0.8 to 0 M. The protein eluted with approximately 0.25 M ammonium sulfate. The extract was concentrated to ∼2 mL by ultrafiltration and purified by gel filtration as described for the other proteins. The purified enzyme was concentrated to 20 mg of protein/mL by ultrafiltration, aliquoted, and stored at −80 °C in 20 mM sodium HEPES buffer (pH 7.5).

The resins used in the protein purifications are cleaned between uses to ensure there is no cross contamination between protein preparations. After each run, the Source Q anion exchange resin is washed with 2 column volumes of 4 M NaCl and subsequently with 2 column volumes of NaOH with the resin stored in 20% ethanol. Both the Phenyl Sepharose and Superdex 200 gel filtration resins are washed with 4 column volumes of 20 mM HEPES (pH 7.5) and subsequently with 6 column volumes of 20% ethanol.

Determination of the Protein Concentration, Purity, and Molecular Mass. Protein concentrations were determined by the Bradford assay using bovine serum albumin as the standard.[23] Sodium dodecyl sulfate−polyacrylamide gel electrophoresis (SDS−PAGE) was performed and the gel stained with Coomassie Blue according to established procedures.[24] The molecular weight of the holoenzymes was determined by gel filtration using a HiLoad 26/60 Superdex 200 prep column.

Preparation of 4-Hydroxy-4-methyl-2-oxoglutarate (HMG). HMG was synthesized chemically as previously described.[5] The substrate was purified by anion exchange chromatography with Dowex Chloride 1X8 resin using a linear gradient from 0 to 0.1 M HCl. Active fractions were pooled, neutralized with NaOH, and lyophilized. The resulting off-white powder was resuspended in minimal dH_2O and desalted by being passed through a P-2 Bio-Gel (Bio-Rad) column (1 cm × 15 cm) with active fractions pooled and lyophilized to a yellow powder. Solutions of HMG were made fresh by resuspending the dry product in minimal dH_2O, the resulting concentration being determined by the amount of pyruvate produced by the HMG/CHA aldolase (using 1.0 mM $CoCl_2$ as a cofactor) from coupling pyruvate formation to NADH oxidation using L-lactate dehydrogenase (LDH).

Metal Substitution. Metal free apoenzymes were prepared by adding 0.5 g of Chelex 100 (Sigma) to 10 mg of purified enzyme in 10 mL of 20 mM sodium HEPES (pH 7.5). After the mixture had been gently stirred for 20 min, Chelex 100 was removed with a 20 μm filter. The apoenzymes were preincubated with the stated metal ions for a minimum of 5 min prior to being used in the kinetic assays.

Enzyme Assays. All kinetic assays were performed in at least duplicate at 25 °C using a Varian Cary 3 spectrophotometer equipped with a thermojacketed cuvette holder. The HMG aldol cleavage and OAA decarboxylase activities were observed by coupling pyruvate formation to NADH oxidation using L-lactate dehydrogenase (LDH). NADH oxidation was monitored at 340 nm, and the extinction coefficient of NADH was determined to be 6220 M^{-1} cm^{-1}. A standard activity assay contained either 1.0 mM HMG or 5.0 mM OAA, 0.4 mM NADH, 1.0 mM $CoCl_2$, and 30 units of LDH in 100 mM HEPES buffer (pH 8.0). Assay reactions were monitored for at least 2 min in the absence of enzyme for the determination of the background rate of degradation of the stated substrate. The enzyme was then added to the reaction mixture, using enzyme pre-equilibrated with the stated metal ion, and monitored for at least 2 min. Enzyme concentrations were added in sufficient quantity to ensure an at least 2-fold change in the rate of substrate turnover compared to the background rate is observed. Enzyme reaction velocities were determined by subtraction of the rate background degradation from the rate observed for the enzyme-catalyzed reaction. All fitting of kinetic data was performed using nonlinear regression in Leonora.[25] All data were fit to the Michaelis−Menten equation. For inhibition assays, the concentration of sodium oxalate was varied from $0.5K_i$ to $5K_i$, and data were fit to a competitive inhibition equation.

Discontinuous end point assays were utilized for the metal ion specificity of Zn^{2+} and Cd^{2+} ions because of the inhibitory effects of these metal ions on LDH. Assays were completed in the absence of LDH and were quenched after 1 min with EDTA before the addition of LDH. The total amount of pyruvate produced over the minute period, relative to controls in the absence of enzyme, was taken as the activity measurement.

Determinations of the Melting Temperature (T_m) by Differential Scanning Calorimetry. Experiments were completed on a MicroCal VP-DSC microcalorimeter. Both the HMG/CHA aldolase and *Tt*RraA were dialyzed into 20 mM HEPES (pH 7.5) and concentrated to 20 mg/mL by ultrafiltration. Enzyme samples were degassed for 5 min before being loaded into a 0.508 mL cell and run against water in the reference cell. A scan rate of 90 °C/h was used for both protein samples. The temperature range was from 10 to 90 °C for the HMG/CHA aldolase and from 10 to 130 °C for *Tt*RraA. Profiles obtained were subtracted from those of control runs containing only buffer.

Structural Comparison and Phylogenetic Analysis. A search for structural homologues of the HMG/CHA aldolase from *P. putida* F1 was completed in DALI[26] and visualized in Pymol.[27] Protein structures containing an rmsd of <3.0 Å were similar in overall size and structure to *Ec*RraA and HMG/CHA aldolase. Sequence conservation among the homologues was mapped onto the HMG/CHA aldolase structure using Consurf[28] and visualized in Pymol. A comprehensive blast search of the NCBI GenBank database using either the HMG/CHA aldolase or *Tt*RraA primary sequences was performed.[29] Representative

Table 1. Comparison of the *P. putida* F1 HMG/CHA Aldolase with the RraA-like Proteins from the PDB

PDB entry	species	rmsd (Å)	% sequence identity (aligned region)	% sequence identity (whole sequence)	% sequence similarity (whole sequence)	motif
3k4i	*P. syringae* pv. *tomato* str. DC3000	1.7	24	17	33	1
2c5q	*S. cerevisiae* S288C	1.9	19	13	25	2
2pcn	*G. kaustophilus* HTA426	2.0	28	17	26	1
1nxj	*M. tuberculosis* H37Rv	2.0	28	16	28	1
3c8o	*P. aeruginosa* PA01	2.1	25	15	29	1
1q5x	*E. coli*	2.1	21	13	23	not applicable
1vi4	*V. cholerae*	2.3	24	15	29	1
1j3l	*T. thermophilus* HB8	2.4	23	15	28	2

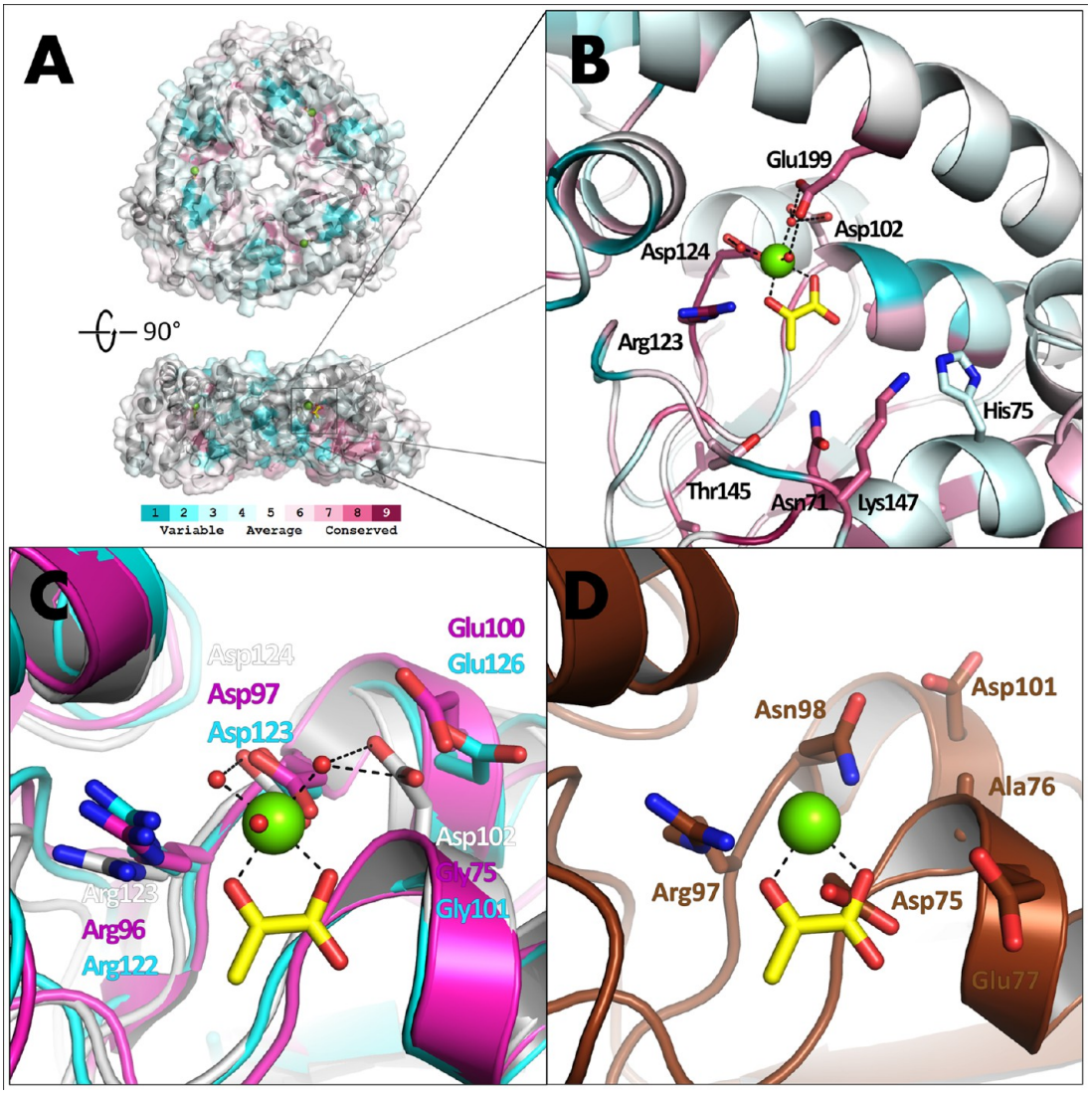

Figure 1. Structural relationship of the HMG/CHA aldolase and RraA-like proteins. (A) Overall structure of the HMG/CHA aldolase and (B) enzyme active site organization, shown with residues colored on the basis of their sequence conservation, using a Consurf color scale,[28] among the RraA-like proteins whose structures have been determined to date. The level of sequence conservation is greatest around the active site pocket of the HMG/CHA aldolase, which contains the bound magnesium ion (green sphere) and pyruvate (yellow sticks). (C) Overlay of structures indicating the different metal binding motifs found in *Tt*RraA (magenta) and Yer010Cp (cyan) (motif 2) vs that found in the HMG/CHA aldolase (white) (motif 1). (D) *Ec*RraA (brown) contains differences in residues vs the sequence found in either active site motif among the RraA-like homologues that would be incompatible with metal and substrate binding.

sequences from across the domains of life were selected to be used in multiple-sequence alignments and the phylogenetic analysis. Alignments and a neighbor joining tree were created using ClustalW2 using a Gonnet scoring matrix with alignments and trees visualized in ESPript and FigTree, respectively.[30,31] Sequences from organisms whose genomes have been sequenced

dx.doi.org/10.1021/bi401486g | *Biochemistry* 2014, 53, 542−553

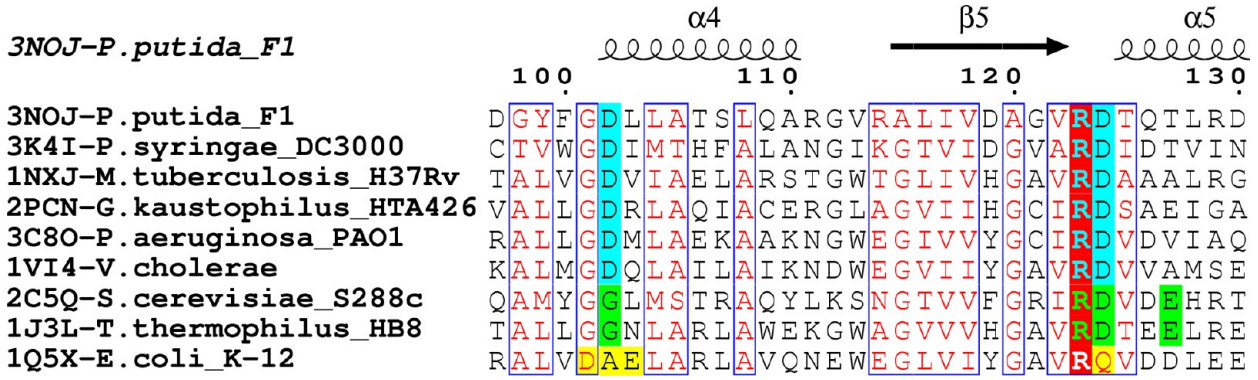

Figure 2. Multiple-sequence alignment of RraA-like homologues showing the metal binding motifs. Aligned sequences are described by their PDB entries and species names. Secondary structural elements (coils for α-helices and an arrow for the β-strand) of the *P. putida* F1 HMG/CHA aldolase are shown above the alignment. Conserved residues in motif 1 (the D-X_{20}-R-D motif) are highlighted in cyan and those in motif 2 [the G-X_{20}-R-D-X_2-(D/E) motif] in green. Sites of residue divergence in *Ec*RraA targeted for mutagenesis are highlighted in yellow.

were also searched for homologues of *E. coli* RNase E and genes from the protocatechuate and gallate *meta* cleavage pathways. Sequences that were found to be part of a multidomain protein or merged with other gene records were omitted.

RESULTS

Bioinformatic Analysis of HMG/CHA Aldolase and RraA Homologues. A DALI search using the *P. putida* F1 HMG/CHA aldolase revealed several proteins of the RraA family to be close structural homologues (Table 1). All of the proteins share a common $\alpha\beta\beta\alpha$ sandwich fold, although they share low levels of sequence identity. Like the HMG/CHA aldolase, the *Ec*RraA and other RraA-like molecules form trimeric biological units through interactions between adjacent monomers.[14,16,17] The majority of these proteins are shorter than the HMG/CHA aldolase by ~30 residues at both the N-terminus and the C-terminus but exhibit conservation in sequences around the known active site of the HMG/CHA aldolase (Figure 1A,B).

Essential for the function of the HMG/CHA aldolase is the coordination of a metal ion to support the binding of a pyruvyl moiety in the class II aldolase. In the structure of the *P. putida* F1 HMG/CHA aldolase, a magnesium ion is coordinated directly or indirectly via water through interactions with Asp102, Asp124, and Glu199 (Figure 1B). The octahedral coordination geometry is completed by interaction with the keto and carboxylate oxygen groups on the bound pyruvate. Asp124 in HMG/CHA aldolase is the only residue observed to be making a direct interaction with bound metal in the aldolase structure and is conserved among most RraA-like family members. This conserved aspartate residue is located beside an arginine residue (Arg123), which has been found to be critical for aldolase/decarboxylase activity in the *P. putida* F1 HMG/CHA aldolase as the positively charged side chain stabilizes the pyruvate enolate intermediate.[5] The Glu199 residue in HMG/CHA aldolase positions one water molecule and in concert with the Asp102 residue positions a second water molecule that coordinate with the bound magnesium ion. The Glu199 residue is present in the *S. cerevisiae* S288C Yer010Cp but is missing in several members of the RraA family, such as the proteins from *E. coli*, *M. tuberculosis*, and *T. thermophilus*, because they lack the C-terminal extension. A residue equivalent to Asp102 is present in all of the RraA-like protein structures except in Yer010Cp and *Tt*RraA. In both *Tt*RraA and Yer010Cp, a glycine residue is found in the position equivalent to Asp102. In the structures of both Yer010Cp and *Tt*RraA, the carboxylate of the glutamate residue, found three residues from the equivalent of the HMG/CHA aldolase Asp124 residue, is observed to occupy a position similar to that of the carboxylate from the HMG/CHA aldolase Asp102 residue (Figure 1C). The minimal side chain of the glycine found at the position equivalent to Asp102 could presumably allow for this alternate metal binding residue to orient into the active site and fulfill the indirect metal binding role in these proteins. Thus, two distinct motifs can be observed in the RraA proteins: a D-X_{20}-R-D motif, herein termed motif 1, and a G-X_{20}-R-D-X_2-(D/E) motif, herein termed motif 2 (Figure 2).

*Ec*RraA appears to be distinct from the other RraA-like proteins in that it does not contain either metal binding motif identified (Figure 1D). The arginine residue found to be essential for activity in the HMG/CHA aldolase (Arg123) is conserved in *Ec*RraA (Arg97). However, the residue equivalent to the conserved metal binding residue in the HMG/CHA aldolase (Asp124) is found to be a glutamine (Gln98) in *Ec*RraA, which would likely not support metal binding. *Ec*RraA is further distinct from either metal binding motif described above because of the presence of an alanine residue (Ala76) in place of either an aspartate in the family containing motif 1 (Asp102 in the HMG/CHA aldolase) or a glycine (Gly75 in the *Tt*RraA) in the family containing motif 2. The *Ec*RraA protein contains an acidic residue (Asp101) similarly found at the end of motif 2, but the presence of a methyl group on the Ala76 residue, which is a glycine in motif 2 of the RraA-like homologues, could sterically restrict this acidic residue from interacting with a metal ion. In addition, a conserved glycine residue among family members that line the bottom of the HMG/CHA aldolase active site pocket is found to be substituted for an aspartate residue (Asp75) in *Ec*RraA. The presence of this aspartate in *Ec*RraA would likely sterically hinder the pyruvyl moiety of a substrate from binding appropriately to the protein. Further, an acidic residue in *Ec*RraA (Glu77) is found close to the metal binding pocket of the protein where acidic residues in the other RraA-like proteins are not found and thus may result in a different metal binding orientation, preventing productive substrate binding leading to catalysis.

Expression and Purification. The *Ec*RraA, *Tt*RraA, and Yer010Cp proteins were overexpressed in *E. coli* BL21(λDE3) and purified by chromatography to homogeneity with a typical yield of ~10 mg of purified protein/L of bacterial culture (Figure 1 of the Supporting Information). The subunit molecular masses of *Ec*RraA, *Tt*RraA, and Yer010Cp were determined by SDS–

dx.doi.org/10.1021/bi401486g | *Biochemistry* 2014, 53, 542−553

Table 2. (A) Relative Activities of the HMG/CHA Aldolase, *Tt*RraA, Yer010Cp, and the *Ec*RraA Variant toward OAA with Various Metal Ions[a] and (B) Relative Activities of the HMG/CHA Aldolase, *Tt*RraA, and Yer010Cp toward HMG with Various Metal Ions[b]

relative activity with OAA (%)							
HMG/CHA aldolase		*Tt*RraA		*Ec*RraA variant		Yer010Cp	
Ni^{2+}	100 ± 0.56	Zn^{2+}	100 ± 6.6	Co^{2+}	100 ± 1.2	Co^{2+}	100 ± 5.8
Co^{2+}	75.0 ± 3.3	Mn^{2+}	57.4 ± 1.6	Mn^{2+}	83.2 ± 3.6	Zn^{2+}	84.4 ± 1.9
Mg^{2+}	39.6 ± 3.5	Co^{2+}	48.0 ± 1.9	Zn^{2+}	34.5 ± 3.8	Ni^{2+}	57.9 ± 3.4
Mn^{2+}	22.6 ± 0.17	Cd^{2+}	38.2 ± 1.1	Ni^{2+}	32.4 ± 3.9	Mg^{2+}	44.1 ± 1.0
Cd^{2+}	4.06 ± 1.64	Ni^{2+}	17.8 ± 1.2	Cd^{2+}	19.2 ± 2.2	Mn^{2+}	40.8 ± 0.80
Zn^{2+}	3.89 ± 0.24	Mg^{2+}	8.67 ± 0.7	Mg^{2+}	8.70 ± 0.46	Cd^{2+}	18.1 ± 0.65
Ca^{2+}	0.164 ± 0.019	Ca^{2+}	0.978 ± 0.061	Ca^{2+}	2.86 ± 0.34	Ca^{2+}	3.78 ± 0.17
apo	0.067 ± 0.006	apo	0.480 ± 0.046	apo	1.46 ± 0.21	apo	0.62 ± 0.0075
EDTA	0.016 ± 0.002	EDTA	0.119 ± 1.9	EDTA	0.443 ± 0.56	EDTA	0.21 ± 0.0020

relative activity with HMG (%)					
HMG/CHA aldolase		*Tt*RraA		Yer010Cp	
Mg^{2+}	100 ± 2.8	Ni^{2+}	100 ± 2.1	Ni^{2+}	100 ± 6.9
Mn^{2+}	90.3 ± 5.7	Co^{2+}	94.4 ± 4.0	Co^{2+}	56.1 ± 0.31
Co^{2+}	64.7 ± 3.6	Zn^{2+}	64.3 ± 5.8	Cd^{2+}	16.6 ± 1.3
Zn^{2+}	49.6 ± 2.7	Cd^{2+}	28.8 ± 3.8	Zn^{2+}	15.4 ± 4.9
Ni^{2+}	28.2 ± 3.4	Mn^{2+}	15.5 ± 0.62	Mg^{2+}	7.45 ± 0.46
Cd^{2+}	5.00 ± 0.20	Mg^{2+}	2.92 ± 0.14	Mn^{2+}	5.42 ± 0.25
Ca^{2+}	ND	Ca^{2+}	1.30 ± 1.8	Ca^{2+}	0.450 ± 0.043
apo	ND	apo	0.201 ± 0.15	apo	0.342 ± 0.081
EDTA	ND	EDTA	0.102 ± 0.051	EDTA	0.0720 ± 0.0010

[a]The activity obtained with the metal resulting in the maximal activity is taken to be 100%. Assays were performed with 5.0 mM OAA, the respective metal chloride salt or EDTA (1.0 mM), 0.3 mM NADH, and 30 units of LDH in 100 mM sodium HEPES buffer (pH 8.0) in a total volume of 1 mL. The activity with Zn^{2+} and Cu^{2+} was determined by the discontinuous method as described in Experimental Procedures. [b]The activity obtained with the metal resulting in the maximal activity is taken to be 100%. Assays were performed with 1.0 mM HMG, the respective metal chloride salt (1.0 mM), 0.3 mM NADH, and 30 units of LDH in 100 mM sodium HEPES buffer (pH 8.0) in a total volume of 1 mL. Values for the HMG/CHA aldolase were taken from ref 5. The activity with Zn^{2+} and Cd^{2+} was determined by the discontinuous method as described in Experimental Procedures. ND means no detectable activity

Table 3. Steady State Kinetic Parameters of the HMG/CHA Aldolase, Yer010Cp, *Tt*RraA, and *Ec*RraA Variant with HMG and OAA[a]

	4-hydroxy-4-methyl-2-oxoglutarate (HMG)			oxaloacetate (OAA)		
enzyme	K_m (μM)	k_{cat} (s^{-1})	k_{cat}/K_m (M^{-1} s^{-1})	K_m (μM)	k_{cat} (s^{-1})	k_{cat}/K_m (M^{-1} s^{-1})
WT HMG/CHA aldolase	187.6 ± 11.0	15.6 ± 0.54	8.3×10^4	297.5 ± 39.6	1.86 ± 0.18	6.2×10^3
E199A HMG/CHA aldolase	708.6 ± 51.9	0.061 ± 0.0026	8.6 × 10	404.7 ± 50.3	0.00139 ± 0.000043	3.4
Yer010Cp	126.5 ± 13.1	0.0276 ± 0.0012	2.1×10^2	132.5 ± 9.58	3.91 ± 0.026	3.0×10^4
*Tt*RraA	150.7 ± 14.1	0.356 ± 0.0085	2.4×10^3	211.4 ± 32.2	1.06 ± 0.0314	5.0×10^3
*Ec*RraA variant	no activity detected above 0.0005 s^{-1}			–	–	1.9 × 10

[a]Assays were completed using 1.0 mM $MgCl_2$ as a cofactor for the wild type and E199A variant of the HMG/CHA aldolase and 1.0 mM $CoCl_2$ as a cofactor for Yer010Cp, *Tt*RraA, and the *Ec*RraA variant.

PAGE and were consistent with the predicted molecular masses of 17.4, 17.0, and 25.0 kDa, respectively.[14−16]

Metal Specificity. *Tt*RraA and Yer010Cp contained both OAA decarboxylase and HMG aldolase activities. The specific activities of the purified apoenzymes with 1 mM metal ions were determined using both 5 mM OAA and 1 mM HMG as substrates. For OAA decarboxylase activity, *Tt*RraA had the highest specific activity for the Zn^{2+} ion whereas Yer010Cp had similar specific activities with Zn^{2+} and Co^{2+} ions (Table 2A). For HMG aldolase activity, however, both *Tt*RraA and Yer010Cp had a preference for Ni^{2+} ions, with Co^{2+} ions being just as effective for aldolase activity in *Tt*RraA (Table 2B). The wild-type *Ec*RraA protein was devoid of either HMG aldolase or OAA decarboxylase activity.

Steady State Kinetic Parameters for OAA Decarboxylase and HMG Aldolase Activities. Using 1.0 mM $CoCl_2$ as a cofactor, the steady state kinetic parameters of both *Tt*RraA and Yer010Cp for both OAA decarboxylase and HMG aldolase activities were determined (Table 3). The *Tt*RraA and Yer010Cp enzymes had kinetic parameters for OAA decarboxylation similar to those of the *P. putida* F1 HMG/CHA aldolase. Yer010Cp and *Tt*RraA also had K_m values for the HMG substrate similar to that of the *P. putida* F1 enzyme. However, relative to that of the HMG/CHA aldolase enzyme, the k_{cat} was reduced in Yer010Cp and *Tt*RraA by 565- and 44-fold, respectively.

Inhibition with Oxalate. The *P. putida* F1 HMG/CHA aldolase is competitively inhibited by oxalate, a pyruvate enolate analogue.[5] The HMG aldolase reaction catalyzed by *Tt*RraA and Yer010Cp was also competitively inhibited by sodium oxalate with K_i values of 37.7 ± 2.3 and 31.9 ± 5.3 μM, respectively, supporting a common mechanism among the enzymes (Figure 2 of the Supporting Information).

dx.doi.org/10.1021/bi401486g | *Biochemistry* 2014, 53, 542−553

Thermostability of *Tt*RraA. Because *T. thermophilus* is a thermophilic bacteria, an attempt to determine the thermostability of *Tt*RraA using DSC was made. Because of limitations with the maximal temperature range of the DSC instrument (130 °C), a defined T_m for *Tt*RraA could not be obtained. However, the T_m for the enzyme is likely close to 130 °C as the progressive decline can just be observed near the instrument's maximal temperature (Figure 3 of the Supporting Information). Comparatively, the T_m for the *P. putida* F1 HMG/CHA aldolase was determined to be 46.5 ± 0.2 °C.

Kinetic Analysis of the HMG/CHA Aldolase Glu199Ala Variant. *Tt*RraA, which lacks the C-terminal portion found on the *P. putida* F1 HMG/CHA aldolase that contains the Glu199 residue that indirectly interacts with the metal cofactor via water molecules, has aldolase activity similar to that of the HMG/CHA aldolase. This suggests that Glu199 is not absolutely required for aldolase activity. To further demonstrate this, we replaced Glu199 of the HMG/CHA aldolase with an alanine by site-specific mutagenesis. Using 1 mM $MgCl_2$ as a cofactor, the k_{cat} of the E199A variant was reduced relative to that of the WT enzyme by 255- and 1338-fold for the HMG aldolase and OAA decarboxylase activities, respectively (Table 3). Relative to that of the WT enzyme, the K_m for $CoCl_2$ increased in the E199A variant by 53-fold to a value similar to that observed for Yer010Cp and *Tt*RraA (Table 4).

Table 4. K_m Values for Co^{2+} in the OAA Decarboxylase Reaction[a]

enzyme	K_m (μM)
WT HMG/CHA aldolase	8.38 ± 0.81
E199A HMG/CHA aldolase	446.3 ± 49
Yer010Cp	113 ± 15
*Tt*RraA	182 ± 24
*Ec*RraA variant	374 ± 37

[a]Assays were completed with 5 mM OAA in 0.1 M sodium HEPES buffer (pH 8.0) with 30 units of LDH, 0.3 mM NADH, and varying concentrations of $CoCl_2$ in a total volume of 1 mL.

Kinetic Analysis of the *Ec*RraA Variant. An attempt to rescue activity in *Ec*RraA, by restoration of motif 2, was made by the introduction of four residue substitutions (D75G/A76G/E77N/Q98D). This *Ec*RraA variant was now capable of catalyzing the OAA decarboxylation but still lacked detectable HMG aldolase activity. The enzyme had a preference for both Co^{2+} and Mn^{2+} ions in the decarboxylase reaction, with all other divalent metals yielding <40% of the activity observed with Co^{2+} (Table 2A). Because of a high K_m for OAA, the *Ec*RraA variant was not able to be saturated with substrate under the conditions used and the k_{cat}/K_m was estimated by a linear plot of activity over substrate concentration. The catalytic efficiency of the *Ec*RraA variant for OAA is approximately 2 orders of magnitude lower relative to those of the other RraA proteins (Table 3). Using 5 mM OAA, the enzyme's K_m for Co^{2+} was found to be 374 ± 37 μM and was higher, but similar, to those of the other enzymes tested (Table 3).

Phylogenetic Analysis. A search of GenBank reveals homologues of the RraA-like family found across all domains of life (Figures 3 and 4). Similarly, RNase E is an endoribonuclease with homologues also found throughout all domains. The majority of the RNase E homologues, however, lack the C-terminal regulatory domain found in the *E. coli* protein, the domain containing the site of RraA binding.[32−34] The lack of an RNase E gene, or an RNase E gene containing a regulatory domain, may suggest that the biological role of the RraA-like gene found within these species may not be to function as an RNase E inhibitor.

Half of the RraA-like gene products surveyed contain a C-terminal extension similar to that found on the *P. putida* F1 HMG/CHA aldolase, which comprises the metal binding Glu199 residue. The other half of the gene products assessed, such as those in *Tt*RraA, are shorter in length, usually comprised of ∼170 residues, and lack a C-terminal extension. Gene products from each domain of life can be found in both the long and short forms. However, all of the gene products from viridiplantae are of the shorter type, whereas all of the fungal gene products are of the longer type. The presence of the C-terminal extension does not correlate with the presence of a particular metal binding motif. Generally, motif 1 is observed in gene products from bacterial and archaeal sources, whereas motif 2 is generally observed in only eukaryotic gene products. There are several exceptions, such as in the gene products from the green algae species *Volvox carteri* and *Ostreococcus tauri* that both contain motif 1 and in *T. thermophilus* HB8, where *Tt*RraA contains motif 2. The presence of the motifs within these species gene products suggests that the proteins can bind divalent metal ions and possess enzymatic activity.

DISCUSSION

An RraA-like gene is found in species from all domains of life. Although many of these organisms lack an identified RNase E or RNase E regulatory domain, they have been annotated as having an RraA function. Structural homology and sequence conservation among the *P. putida* F1 HMG/CHA aldolase and the RraA-like protein structures determined to date have suggested that many members of the RraA-like family may contain aldolase and/or decarboxylase activity. Comparative analysis of the metal binding residues in the *P. putida* F1 HMG/CHA aldolase and the homologous RraA-like structures has revealed the potential for a different metal binding motif (motif 2) within some members of the family that differs from that observed in the HMG/CHA aldolase. Sequence analysis indicates that, among the members of the RraA-like family, motif 1 (the motif found in the HMG/CHA aldolase) is generally found in members from bacterial and archaeal species, whereas motif 2 is generally found in gene products from eukaryotic species. The presence of HMG aldolase and OAA decarboxylase activity in Yer010Cp and *Tt*RraA, both of which contain motif 2, substantiates the proposal that motif 2 is able to support metal binding and enzymatic activity within these proteins. Both Yer010Cp and *Tt*RraA had kinetic parameters for OAA decarboxylation similar to those of *P. putida* F1 HMG/CHA aldolase, but they had reduced catalytic efficiencies for their HMG aldolase activity, relative to that of the *P. putida* F1 enzyme (43- and 565-fold decreases in k_{cat}, respectively). This decrease in k_{cat} may be due to differences in the metal binding motifs and/or small changes to conserved residues within the active site pocket of the respective enzymes.

Proteins of the RraA-like family can also be separated into two groups based on the size of the gene product. Members of the long form group, including the *P. putida* F1 HMG/CHA aldolase and Yer010Cp, contain ∼230 residues, and members of the short form group, including *Ec*RraA and *Tt*RraA, contain ∼170 residues. The presence of the C-terminal extension does not correlate with the presence of a particular binding motif, and both short and long forms are observed in all domains of life. To date, only *Ec*RraA and an RraA from *V. vulnificus* (RraAV1), both

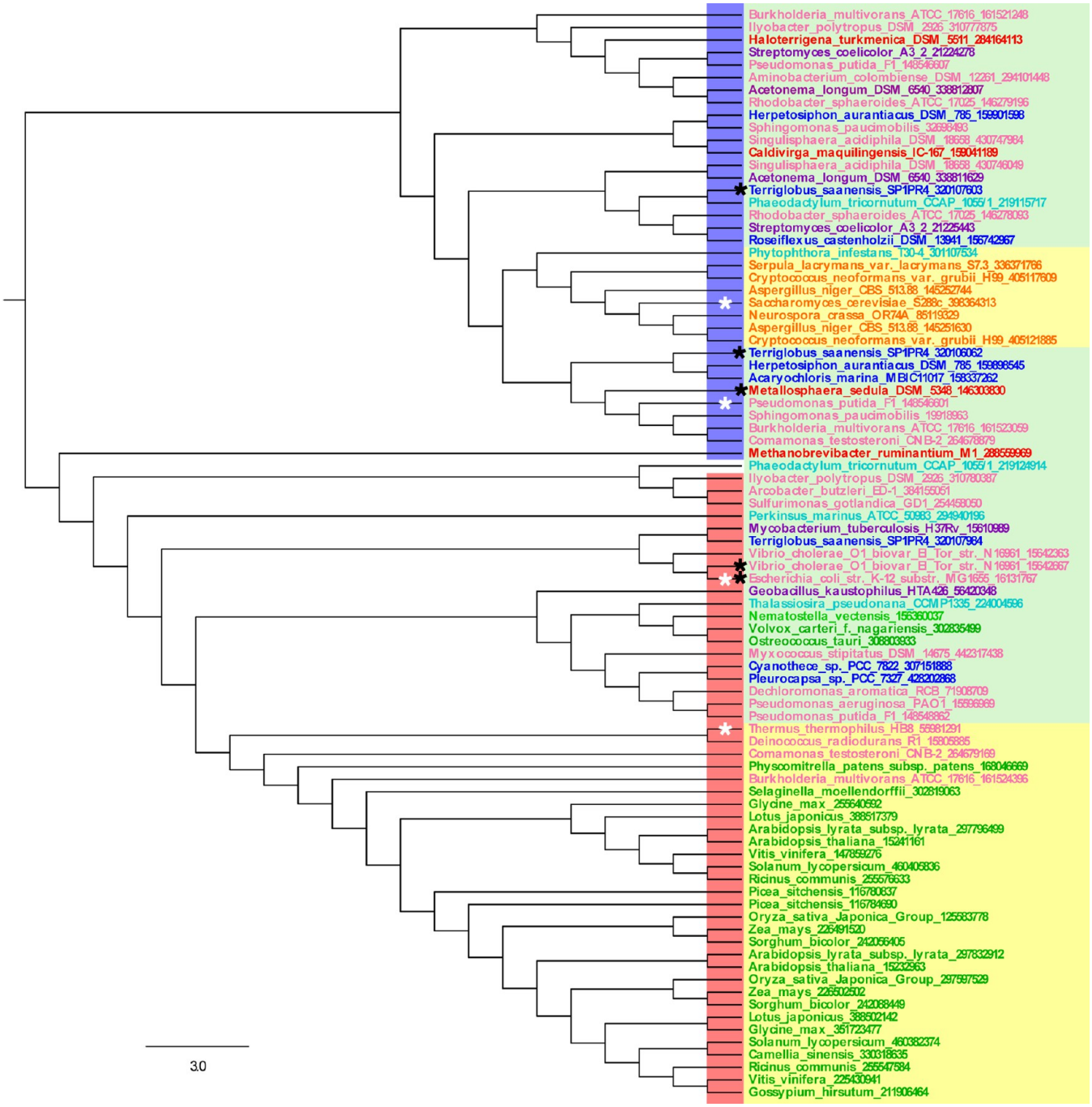

Figure 3. Phylogenetic tree of the HMG/CHA aldolase and RraA-like homologues. Gene products from Gram-positive bacteria are colored purple, those from Gram-negative bacteria pink, those from ungrouped bacteria blue, those from viridiplantae green, those from fungi orange, those from stramenopiles cyan, and those from archaea red. Gene products containing a C-terminal extension comprising an acidic residue equivalent to the Glu199 metal binding residue of the HMG/CHA aldolase are preceded by a blue box. Those lacking the extension are preceded by a red box. The second gene product from *Phaeodactylum tricornutum* (Gene ID 219124914) contains a C-terminal extension that is dissimilar from the other members and lacks an equivalent acidic residue. The metal binding motifs among the gene products are indicated by background shading, with members having the G-X_{20}-R-D-X_2-(D/E) motif highlighted in yellow and members with the D-X_{20}-R-D motif highlighted in green. A black asterisk indicates gene products that, as observed with the *Ec*RraA, have residue substitutions within the motif that would hinder metal binding and enzymatic activity. White asterisks denote gene products characterized in this study.

members of the short form group, have been characterized as containing RNase E inhibitory function.[9,11,19] The *P. putida* F1 HMG/CHA aldolase Glu199 residue, involved in positioning metal-ligating water molecules in the aldolase structure, is found on the C-terminal extension that is absent in the shorter RraA-like family members. Among the RraA-like homologues that contain a C-terminal extension, an acidic residue equivalent to the HMG/CHA aldolase Glu199 residue is found to be conserved. When Glu199 was replaced with alanine, the *P. putida* F1 enzyme was still capable of catalyzing both the aldolase and decarboxylase reactions. However, the K_m for Co^{2+} increased for the E199A variant relative to that of the wild type for the OAA

dx.doi.org/10.1021/bi401486g | *Biochemistry* 2014, 53, 542−553

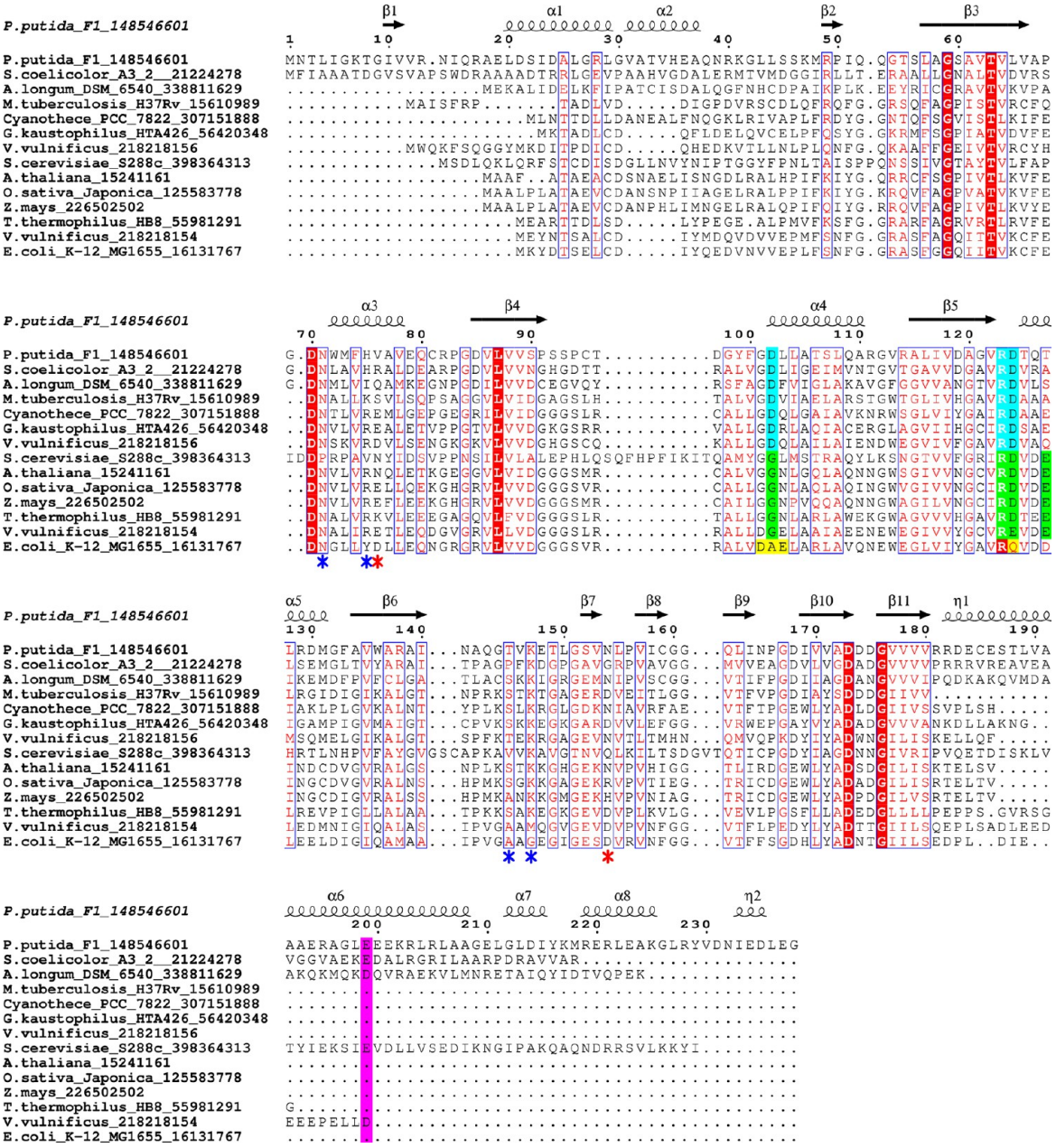

Figure 4. Sequence alignment of HMG/CHA aldolase and RraA-like homologues. Fully conserved residues are shown in white text with a red background and similar residues are shown in red text. Secondary structural elements (coils for α-helices and arrows for β-strands) of the *P. putida* F1 HMG/CHA aldolase are shown above the alignment. The different residues representing metal binding motifs D-X_{20}-R-D (cyan) and G-X_{20}-R-D-X_2-(D/E) (green) are highlighted. The Glu199 metal binding residue from the HMG/CHA aldolase and its homologues is highlighted in magenta. Sites of residue divergence in *Ec*RraA targeted for mutagenesis are highlighted in yellow. Aligned sequences are described by their species name and GI numbers. Asterisks denote either residues located in the active site pocket of the aldolase (blue) or residues on *Ec*RraA observed to interact with SrmB (red).

reaction, indicating that although it is not essential for metal binding and catalysis, the presence of the Glu199 residue enhances the enzyme's metal binding ability. The presence of aldolase and decarboxylase activity in *Tt*RraA, which lacks this C-terminal extension, signifies that a metal binding residue at this position is not absolutely required. Furthermore, the lack of the C-terminal extension in *Tt*RraA indicates that this terminal portion found on the *P. putida* F1 enzyme, Yer010Cp, and other long form RraA-like homologues is not required for catalytic activity and its presence as a distinguishing feature of the RraA family is insignificant.

Similar to HMG/CHA aldolase, *Tt*RraA and Yer010Cp required a divalent metal ion for their activity, and their aldolase reaction was competitively inhibited by oxalate, a pyruvate enolate analogue, suggesting a common catalytic mechanism among the enzymes. The metal ion specificity among the proteins was, however, different. The difference in metal ion specificity is likely attributed to differences in the metal binding residues. However, the rationale for why the metal preference is different between substrates, HMG or OAA, for an individual enzyme is not clear. In the HMG/CHA aldolase aldol cleavage reaction, it has been proposed that the bound divalent ion acts as a Lewis base to promote a metal-bound water to act as the general base deprotonating the substrate C4-hydroxyl initiating the reaction.[5] In this situation, it could be rationalized that each coordinated metal would vary in its ability to promote water as a

dx.doi.org/10.1021/bi401486g | *Biochemistry* 2014, 53, 542−553

general base. This mechanism contrasts with that proposed for the OAA decarboxylation reaction where no general base is thought to be required. With OAA decarboxylation, the metal would be required only to facilitate polarization of the pyruvyl moiety.

Unlike *Tt*RraA and Yer010Cp, *Ec*RraA was devoid of either HMG aldolase or OAA decarboxylase activity. An attempt to rescue activity in *Ec*RraA was made by incorporating motif 2 within the protein. The *Ec*RraA variant was able to catalyze OAA decarboxylation, supporting the role of this motif in enzyme function. The variant, however, still lacked detectable HMG aldol lyase activity. *Ec*RraA contains several other residue substitutions from what is conserved among the family members in the pyruvate binding pocket (Figure 4). In particular, residue changes along the periphery of the binding pocket, including a conserved lysine (Lys120 in *Tt*RraA), either a serine or threonine (Ser118 in *Tt*RraA), and either an arginine or histidine (Arg48 in *Tt*RraA), are found to be a glycine, alanine, and tyrosine in *Ec*RraA, respectively (Figure 4). Although the role of these conserved residues in the function of aldolases has yet to be elucidated, it is possible that some of these residue changes in the *Ec*RraA prevent the HMG aldol substrate from binding appropriately.

The identification of *Ec*RraA as an inhibitor of RNase E has prompted the hypothesis that the RraA-like homologues may contain this function in the other species. Although many species with an RraA-like gene contain an RNase E homologue, most of those homologues contain only the catalytic domain of RNase E or a regulatory domain dissimilar to that of the *E. coli* protein.[32−34] Alternatively, in Pseudomonads and Sphingomonads, the RraA-like gene is commonly found as part of an operon for the *meta* cleavage of the aromatic substrate protocatechuate or gallate.[2,3] Outside of the Pseudomonads and Sphingomonads, however, the RraA-like genes are commonly found in species that do not contain genes known for the *meta* cleavage of protocatechuate or gallate. Some species such as *E. coli*, *Burkholderia xenovorans* LB400, and *M. tuberculosis* H37Rv that contain RraA-like genes also contain genes for the *meta* cleavage of other aromatic and cyclic compounds such as hydoxyphenyl acetate, biphenyl, and cholesterol metabolites, respectively.[35−37] The *meta* cleavage pathway for these compounds also leads to a 4-hydroxy-2-oxo acid compound that could be utilized by the RraA-like gene. However, the genes for the *meta* cleavage of these compounds, and for the *meta* cleavage of protocatechuate and gallate, are found in gene clusters comprising all of the genes, including a class II aldolase, required for complete degradation of the specific aromatic compound.[7,38,39] Further, HMG/CHA aldolases have been observed to contain substrate specificity toward substrates containing a C4 carboxylate moiety that has been observed to be produced only through the *meta* cleavage pathways of protocatechuate and gallate.[3−5] Therefore, it is unlikely that the RraA-like gene is present in those species to act as a member of those *meta* cleavage pathways already defined. *Tt*RraA from *T. thermophilus* HB8 and Yer010Cp from *S. cerevisiae* S288C, two species that lack both a defined RNase E and genes related to the protocatechuate or gallate *meta* cleavage pathways, have HMG aldolase activity with kinetic parameters similar to that of the characterized HMG/CHA aldolases.[4,5] *Tt*RraA was found to be thermostable ($T_m \sim 130$ °C) and when heat treated at 95 °C for 1 h maintained its specific activity for both the HMG and OAA substrates (data not shown). The thermostability of *Tt*RraA suggests that the protein is adept to environments inhabited by *T. thermophilus* HB8 and may maintain enzymatic activity within the organism. The enzymatic activity conserved in *Tt*RraA, Yer010Cp, and possibly in the other RraA-like family members may suggest that these genes are members of an undescribed metabolic pathway conserved across the domains of life.

It is interesting to note that while a majority of HMG/CHA aldolases characterized have been from bacterial species, the original identification and characterization of the HMG/CHA aldolase enzyme was conducted with extracts of germinating peanut cotyledons.[40] Although the complete genome of *Arachis hypogaea* has yet to be elucidated, the presence of RraA-like genes within viridiplantae appears to be widespread. In *Arabidopsis thaliana*, three copies of an RraA-like gene that is >40% identical to *Ec*RraA are found within its genome (AT5G56260, AT5G16450, and AT3G02770). The *A. thaliana* RraA-like gene products also contain considerable sequence conservation of residues found within the active site pocket of the HMG/CHA aldolase and thus may support an aldolase reaction with substrate specificities similar to those of the *P. putida* F1 enzyme (Figure 4). All three copies, like the rest of gene copies in viridiplantae, contain metal binding motif 2, which would support metal binding and enzymatic activity within these proteins. Expression studies in *A. thaliana* have revealed that transcripts of these RraA-like genes are produced in many cell types and during different stages of development.[41] Although individual knockouts of these RraA-like genes exist in *A. thaliana*, phenotypes resulting from their knockouts have yet to be characterized.[42] It is unlikely that the individual knockouts will produce a significant phenotype as the high degree of homology of the three copies found in *A. thaliana* will likely result in redundancy of function.

The molecular determinants of the *Ec*RraA involved with the interaction with the RNase E regulatory domain have yet to be elucidated. However, *Ec*RraA has also been observed to bind to and inhibit ATP-dependent DEAD-box RNA helicases, and recent cocrystal structures of *Ec*RraA in complex with a fragment of RhlB (PDB entry 2YJV) and the full length SrmB (PDB entry 2YJT) have been submitted to the PDB. The sites of interaction with *Ec*RraA overlap in the two cocrystal structures, and Asp50, Glu53, and Asp128 of *Ec*RraA were shown to be critical for forming salt bridges with arginine residues on SrmB.[12] *V. vulnificus* encodes two RraA-like genes within its genome, RraAV1 and RraAV2, with the RraAV1, but not the RraAV2, exhibiting *E. coli* RNase E inhibitory ability.[19] All three acidic residues found in *Ec*RraA that form the interaction with SrmB are conserved in RraAV1 (Figure 4). RraAV2, on the other hand, has serine and asparagine substitutions at the equivalent *Ec*RraA Glu53 and Asp128 positions, respectively. *Ec*RraA is known to interact with RNase E through locations on the regulatory domain containing stretches of mainly basic residues.[11] It is possible that the interactions observed in the *Ec*RraA−SrmB complex may be conserved with interaction with RNase E, and the residue substitutions observed in RraAV2 may hinder that interaction. Among the RraA-like homologues, there is minimal sequence conservation at the sites of the *Ec*RraA interacting residue locations. There is, however, conservation of hydrophilic residues at these locations that may be a result of species-specific interactions with their binding partners or a loss of function. In both *Ec*RraA cocrystal structures, the site of protein−protein interaction between *Ec*RraA and the helicase is found on the surface of the protein close to, but not including, residues found within the active site pocket of the RraA. As such, these interactions would likely be distinct from the catalytic activity in other RraA homologues that are enzymatically active. *Ec*RraA has

dx.doi.org/10.1021/bi401486g | *Biochemistry* 2014, 53, 542−553

been observed to bind RNase E in the absence of divalent metals.[11] Several structures of RraA-like proteins that lack a bound divalent metal ion have been determined, and here it was shown that *Tt*RraA, Yer010Cp, and the *Ec*RraA variant were stable in the absence of a divalent metal and could be reconstituted leading to a catalytically active enzyme. Thus, the ability of the RraA family members comprising a metal ion binding motif to bind divalent metals is likely not required for a structural role or to facilitate protein−protein interactions in these proteins but is unique to the potential class II aldolase activity.

We have provided evidence that many of the RraA-like proteins contain aldolase and/or decarboxylase activity either in place of or in addition to the RNase E inhibitor functions previously noted. We suggest that future annotations of members of this family be termed aldolase$_{II}$/RraA to reflect the potential activities of a class II aldolase and an inhibitor of RNA turnover.

■ ASSOCIATED CONTENT

Supporting Information

Figures describing SDS−PAGE purity analysis of *Ec*RraA, *Tt*RraA, and Yer010Cp purifications, Lineweaver−Burke plots of sodium oxalate inhibition, and DSC thermostability analysis. This material is available free of charge via the Internet at http://pubs.acs.org.

■ AUTHOR INFORMATION

Corresponding Author

*Department of Molecular and Cellular Biology, University of Guelph, Guelph, Ontario, Canada N1G 5E9. E-mail: sseah@uoguelph.ca. Phone: (519) 824-4120, ext. 56750. Fax: (519) 837-1802.

Funding

This research is supported by National Science and Engineering Research Council of Canada Grant 238284 (to S.Y.K.S.).

Notes

The authors declare no competing financial interest.

■ ACKNOWLEDGMENTS

We thank Brian Bryska, Douglas Grahame, and Dr. Rickey Yada for their help and support with the DSC experiments.

■ ABBREVIATIONS

HEPES, 4-(2-hydroxyethyl)-1-piperazinepropanesulfonic acid; IPTG, isopropyl β-D-thiogalactopyranoside; LDH, L-lactate dehydrogenase; OAA, oxaloacetate; HMG, 4-hydroxy-4-methyl-2-oxoglutarate; CHA, 4-carboxy-4-hydroxy-2-oxoadipate; rmsd, root-mean-square deviation.

■ REFERENCES

(1) Dagley, S., Geary, P. J., and Wood, J. M. (1968) The metabolism of protocatechuate by *Pseudomonas testosteroni*. *Biochem. J. 109*, 559−568.

(2) Nogales, J., Canales, A., Jimenez-Barbero, J., Serra, B., Pingarron, J. M., Garcia, J. L., and Diaz, E. (2011) Unravelling the gallic acid degradation pathway in bacteria: The gal cluster from *Pseudomonas putida*. *Mol. Microbiol. 79*, 359−374.

(3) Hara, H., Masai, E., Miyauchi, K., Katayama, Y., and Fukuda, M. (2003) Characterization of the 4-carboxy-4-hydroxy-2-oxoadipate aldolase gene and operon structure of the protocatechuate 4,5-cleavage pathway genes in *Sphingomonas paucimobilis* SYK-6. *J. Bacteriol. 185*, 41−50.

(4) Maruyama, K. (1990) Purification and properties of 4-hydroxy-4-methyl-2-oxoglutarate aldolase from *Pseudomonas ochraceae* grown on phthalate. *J. Biochem. 108*, 327−333.

(5) Wang, W., Mazurkewich, S., Kimber, M. S., and Seah, S. Y. (2010) Structural and kinetic characterization of 4-hydroxy-4-methyl-2-oxoglutarate/4-carboxy-4-hydroxy-2-oxoadipate aldolase, a protocatechuate degradation enzyme evolutionarily convergent with the HpaI and DmpG pyruvate aldolases. *J. Biol. Chem. 285*, 36608−36615.

(6) Manjasetty, B. A., Powlowski, J., and Vrielink, A. (2003) Crystal structure of a bifunctional aldolase-dehydrogenase: Sequestering a reactive and volatile intermediate. *Proc. Natl. Acad. Sci. U.S.A. 100*, 6992−6997.

(7) Carere, J., McKenna, S. E., Kimber, M. S., and Seah, S. Y. (2013) Characterization of an aldolase-dehydrogenase complex from the cholesterol degradation pathway of *Mycobacterium tuberculosis*. *Biochemistry 52*, 3502−3511.

(8) Rea, D., Fulop, V., Bugg, T. D., and Roper, D. I. (2007) Structure and mechanism of HpcH: A metal ion dependent class II aldolase from the homoprotocatechuate degradation pathway of *Escherichia coli*. *J. Mol. Biol. 373*, 866−876.

(9) Lee, K., Zhan, X., Gao, J., Qiu, J., Feng, Y., Meganathan, R., Cohen, S. N., and Georgiou, G. (2003) RraA. A protein inhibitor of RNase E activity that globally modulates RNA abundance in *E. coli*. *Cell 114*, 623−634.

(10) Gorna, M. W., Carpousis, A. J., and Luisi, B. F. (2012) From conformational chaos to robust regulation: The structure and function of the multi-enzyme RNA degradosome. *Q. Rev. Biophys. 45*, 105−145.

(11) Gorna, M. W., Pietras, Z., Tsai, Y. C., Callaghan, A. J., Hernandez, H., Robinson, C. V., and Luisi, B. F. (2010) The regulatory protein RraA modulates RNA-binding and helicase activities of the *E. coli* RNA degradosome. *RNA 16*, 553−562.

(12) Pietras, Z., Hardwick, S. W., Swiezewski, S., and Luisi, B. F. (2013) Potential regulatory interactions of *Escherichia coli* RraA protein with DEAD-box helicases. *J. Biol. Chem. 288*, 31919−31929.

(13) Coburn, G. A., Miao, X., Briant, D. J., and Mackie, G. A. (1999) Reconstitution of a minimal RNA degradosome demonstrates functional coordination between a 3′ exonuclease and a DEAD-box RNA helicase. *Genes Dev. 13*, 2594−2603.

(14) Monzingo, A. F., Gao, J., Qiu, J., Georgiou, G., and Robertus, J. D. (2003) The X-ray structure of *Escherichia coli* RraA (MenG), a protein inhibitor of RNA processing. *J. Mol. Biol. 332*, 1015−1024.

(15) Rehse, P. H., Kuroishi, C., and Tahirov, T. H. (2004) Structure of the RNA-processing inhibitor RraA from *Thermus thermophilis*. *Acta Crystallogr. D60*, 1997−2002.

(16) Leulliot, N., Quevillon-Cheruel, S., Graille, M., Schiltz, M., Blondeau, K., Janin, J., and Van Tilbeurgh, H. (2005) Crystal structure of yeast YER010Cp, a knotable member of the RraA protein family. *Protein Sci. 14*, 2751−2758.

(17) Johnston, J. M., Arcus, V. L., Morton, C. J., Parker, M. W., and Baker, E. N. (2003) Crystal structure of a putative methyltransferase from *Mycobacterium tuberculosis*: Misannotation of a genome clarified by protein structural analysis. *J. Bacteriol. 185*, 4057−4065.

(18) Badger, J., Sauder, J. M., Adams, J. M., Antonysamy, S., Bain, K., Bergseid, M. G., Buchanan, S. G., Buchanan, M. D., Batiyenko, Y., Christopher, J. A., Emtage, S., Eroshkina, A., Feil, I., Furlong, E. B., Gajiwala, K. S., Gao, X., He, D., Hendle, J., Huber, A., Hoda, K., Kearins, P., Kissinger, C., Laubert, B., Lewis, H. A., Lin, J., Loomis, K., Lorimer, D., Louie, G., Maletic, M., Marsh, C. D., Miller, I., Molinari, J., Muller-Dieckmann, H. J., Newman, J. M., Noland, B. W., Pagarigan, B., Park, F., Peat, T. S., Post, K. W., Radojicic, S., Ramos, A., Romero, R., Rutter, M. E., Sanderson, W. E., Schwinn, K. D., Tresser, J., Winhoven, J., Wright, T. A., Wu, L., Xu, J., and Harris, T. J. (2005) Structural analysis of a set of proteins resulting from a bacterial genomics project. *Proteins 60*, 787−796.

(19) Lee, M., Yeom, J. H., Sim, S. H., Ahn, S., and Lee, K. (2009) Effects of *Escherichia coli* RraA orthologs of *Vibrio vulnificus* on the ribonucleolytic activity of RNase E *in vivo*. *Curr. Microbiol. 58*, 349−353.

(20) Yokoyama, S., Hirota, H., Kigawa, T., Yabuki, T., Shirouzu, M., Terada, T., Ito, Y., Matsuo, Y., Kuroda, Y., Nishimura, Y., Kyogoku, Y.,

Miki, K., Masui, R., and Kuramitsu, S. (2000) Structural genomics projects in japan. *Nat. Struct. Biol. 7* (Suppl.), 943−945.
(21) Tabor, S., and Richardson, C. C. (1985) A bacteriophage T7 RNA polymerase/promoter system for controlled exclusive expression of specific genes. *Proc. Natl. Acad. Sci. U.S.A. 82*, 1074−1078.
(22) Liu, H., and Naismith, J. H. (2008) An efficient one-step site-directed deletion, insertion, single and multiple-site plasmid mutagenesis protocol. *BMC Biotechnol. 8* (91), 6750-8-91.
(23) Bradford, M. M. (1976) A rapid and sensitive method for the quantitation of microgram quantities of protein utilizing the principle of protein-dye binding. *Anal. Biochem. 72*, 248−254.
(24) Laemmli, U. K. (1970) Cleavage of structural proteins during the assembly of the head of bacteriophage T4. *Nature 227*, 680−685.
(25) Cornish-Bowden, A. (1995) *Analysis of enzyme kinetic data*, Oxford University Press, New York.
(26) Holm, L., and Rosenstrom, P. (2010) Dali server: Conservation mapping in 3D. *Nucleic Acids Res. 38*, W545−W549.
(27) DeLano, W. L. (2002) *The PyMOL molecular graphics system*, version 1.4.1, Schrödinger, LLC, Portland, OR.
(28) Landau, M., Mayrose, I., Rosenberg, Y., Glaser, F., Martz, E., Pupko, T., and Ben-Tal, N. (2005) ConSurf 2005: The projection of evolutionary conservation scores of residues on protein structures. *Nucleic Acids Res. 33*, W299−W302.
(29) Altschul, S. F., Gish, W., Miller, W., Myers, E. W., and Lipman, D. J. (1990) Basic local alignment search tool. *J. Mol. Biol. 215*, 403−410.
(30) Aiyar, A. (2000) The use of CLUSTAL W and CLUSTAL X for multiple sequence alignment. *Methods Mol. Biol. 132*, 221−241.
(31) Gouet, P., Courcelle, E., Stuart, D. I., and Metoz, F. (1999) ESPript: Analysis of multiple sequence alignments in PostScript. *Bioinformatics 15*, 305−308.
(32) Schein, A., Sheffy-Levin, S., Glaser, F., and Schuster, G. (2008) The RNase E/G-type endoribonuclease of higher plants is located in the chloroplast and cleaves RNA similarly to the *E. coli* enzyme. *RNA 14*, 1057−1068.
(33) Lee, K., and Cohen, S. N. (2003) A *Streptomyces coelicolor* functional orthologue of *Escherichia coli* RNase E shows shuffling of catalytic and PNPase-binding domains. *Mol. Microbiol. 48*, 349−360.
(34) Kaberdin, V. R., Miczak, A., Jakobsen, J. S., Lin-Chao, S., McDowall, K. J., and von Gabain, A. (1998) The endoribonucleolytic N-terminal half of *Escherichia coli* RNase E is evolutionarily conserved in *Synechocystis* sp. and other bacteria but not the C-terminal half, which is sufficient for degradosome assembly. *Proc. Natl. Acad. Sci. U.S.A. 95*, 11637−11642.
(35) Jenkins, J. R., and Cooper, R. A. (1988) Molecular cloning, expression, and analysis of the genes of the homoprotocatechuate catabolic pathway of *Escherichia coli* C. *J. Bacteriol. 170*, 5317−5324.
(36) Denef, V. J., Patrauchan, M. A., Florizone, C., Park, J., Tsoi, T. V., Verstraete, W., Tiedje, J. M., and Eltis, L. D. (2005) Growth substrate- and phase-specific expression of biphenyl, benzoate, and C1 metabolic pathways in *Burkholderia xenovorans* LB400. *J. Bacteriol. 187*, 7996−8005.
(37) Van der Geize, R., Yam, K., Heuser, T., Wilbrink, M. H., Hara, H., Anderton, M. C., Sim, E., Dijkhuizen, L., Davies, J. E., Mohn, W. W., and Eltis, L. D. (2007) A gene cluster encoding cholesterol catabolism in a soil actinomycete provides insight into *Mycobacterium tuberculosis* survival in macrophages. *Proc. Natl. Acad. Sci. U.S.A. 104*, 1947−1952.
(38) Wang, W., and Seah, S. Y. (2005) Purification and biochemical characterization of a pyruvate-specific class II aldolase, HpaI. *Biochemistry 44*, 9447−9455.
(39) Baker, P., Pan, D., Carere, J., Rossi, A., Wang, W., and Seah, S. Y. (2009) Characterization of an aldolase-dehydrogenase complex that exhibits substrate channeling in the polychlorinated biphenyls degradation pathway. *Biochemistry 48*, 6551−6558.
(40) Shannon, L. M., and Marcus, A. (1962) γ-Methyl-γ-hydroxy-α-ketoglutaric aldolase. I. Purification and properties. *J. Biol. Chem. 237*, 3342−3347.
(41) Schmid, M., Davison, T. S., Henz, S. R., Pape, U. J., Demar, M., Vingron, M., Scholkopf, B., Weigel, D., and Lohmann, J. U. (2005) A gene expression map of *Arabidopsis thaliana* development. *Nat. Genet. 37*, 501−506.
(42) Alonso, J. M., Stepanova, A. N., Leisse, T. J., Kim, C. J., Chen, H., Shinn, P., Stevenson, D. K., Zimmerman, J., Barajas, P., Cheuk, R., Gadrinab, C., Heller, C., Jeske, A., Koesema, E., Meyers, C. C., Parker, H., Prednis, L., Ansari, Y., Choy, N., Deen, H., Geralt, M., Hazari, N., Hom, E., Karnes, M., Mulholland, C., Ndubaku, R., Schmidt, I., Guzman, P., Aguilar-Henonin, L., Schmid, M., Weigel, D., Carter, D. E., Marchand, T., Risseeuw, E., Brogden, D., Zeko, A., Crosby, W. L., Berry, C. C., and Ecker, J. R. (2003) Genome-wide insertional mutagenesis of *Arabidopsis thaliana*. *Science 301*, 653−657.